

η photoproduction in the resonance energy region. *

V. Shklyar,[†] H. Lenske, and U. Mosel

Institut für Theoretische Physik, Universität Giessen, D-35392 Giessen, Germany

The η production in the nucleon resonance energy region is studied within the unitary coupled-channels effective Lagrangian approach of the Giessen model. We demonstrate that the second peak recently observed in the cross section of η photoproduction on the neutron at $\sqrt{s}=1.66$ GeV can be explained in terms of coupled-channel effects due to $S_{11}(1650)$ and $P_{11}(1710)$ resonance excitations.

PACS numbers: 11.80.-m, 13.75.Gx, 14.20.Gk, 13.30.Gk

Most of the information about the electromagnetic properties of nucleon resonances comes from the analysis of pion photoproduction data. However, since we have to expect that not all of the resonances couple equally strong to the πN channel other production and decay scenarios must be investigated. Such a complementary information on resonance spectra can be obtained from the study of reactions with $K\Lambda$, ηN , ωN etc. in the final state. Recently, $K\Lambda$ photoproduction has attracted considerable attention [1, 2, 3, 4] in prospects of searching for 'hidden' states predicted in [5, 6, 7]. The η production on the neutron might be of particular interest for the search of narrow 'hidden' states predicted by some quark models [8, 9]. Due to the isoscalar nature of the η meson this reaction selects only isospin- $\frac{1}{2}$ channel which also simplifies the analysis. The previous experimental studies of γd scattering [10, 11] have shown that η photoproduction on the neutron at c.m. energies up to $\sqrt{s}=1.6$ GeV is governed by the excitation of the $S_{11}(1535)$ resonance. Recently, the GRAAL [12] and CBELSA-TAPS [13] collaborations reported on their preliminary $\gamma n \rightarrow \eta n$ data which has been extracted from the analysis of γd scattering. Although these measurements need to be confirmed a striking and unexpected result of these findings is that the integrated neutron cross section has an additional maximum at c.m. energy around $\sqrt{s}=1.66$ GeV. To our knowledge a consistent explanation of this phenomenon is pending.

The central question is whether the observed structure comes from the excitation of an unknown baryonic state. In [14] the existence of a narrow resonance with the mass $M=1.675$ GeV and strong coupling to the ηn final state has been predicted. The contribution from this resonance has been proposed [15] as an explanation of the peak seen in the preliminary $\gamma n^* \rightarrow \eta n$ GRAAL data [12] at $\sqrt{s}=1.6\ldots 1.7$ GeV. However, before any conclusion can be drawn the conventional mechanisms in the η photoproduction both on the proton and on the neutron has to be investigated in detail. In this letter we present a first attempt for a multichannel analysis of ηp and ηn reactions within the Giessen Model, a unitary coupled-channel approach taking into account constraints from the other scattering channels. The Giessen model [16, 17, 18] has been developed for the simultaneous analysis of the pion- and photon-induced reactions up to about 2 GeV. In [4, 19] an updated solution of the coupled-channel problem has been obtained to $\pi N \rightarrow \pi N, 2\pi N, \eta N, \omega N, K\Lambda, K\Sigma$ and $\gamma N \rightarrow \gamma N, \pi N, \eta N, \omega N, K\Lambda, K\Sigma$ reactions at energies from the threshold up to 2 GeV. At that time the η photoproduction on the neutron was beyond the scope of the calculations. Since the hadronic resonance parameters have been extracted in [4, 19] the extension of the model to $\gamma n \rightarrow \eta n$ is in principle straightforward if the neutron helicity amplitudes of all resonances would be known. The electromagnetic properties of most of the discovered states were extracted only from the analysis of the pion photoproduction data. Hence, the uncertainties of the extracted parameters would bring a large ambiguity to such a calculations.

A very important example relevant for the case at hand are the electromagnetic properties of the $S_{11}(1535)$ resonance. Because of the strong coupling of this state to ηN , the amplitude ratio $R = A_{1/2}^n(S_{11}(1535))/A_{1/2}^p(S_{11}(1535))$ defines a balance between η meson photoproduction on the neutron and the proton at energies close to this resonance mass. The various analyses of pion photoproduction find this ratio being spread over a wide range $R = -0.3 \ldots -1$ (see the Particle Data Group (PDG) [20] and references therein). On the other hand the combined studies of the ηp and ηn photoproduction data [21, 22, 23, 24] seems to agree on the value $R \approx -0.8$. Hence, one can hope that the multichannel analysis of the πN - and ηN -channels maximally constrains the resonance parameters, thereby a solid conclusion on the reaction mechanism and resonance parameters can be drawn.

The aim of this letter is as follows. We repeat our previous calculations [4, 19] but taking into account presently available ηn data to constrain the couplings $N^* \rightarrow \gamma n$. Using the hadronic parameters from [19] we predict the angular distribution and beam asymmetry for $\gamma n \rightarrow \eta n$ scattering in the energy region where the second peak in the ηn data is observed.

* Supported by Forschungszentrum Juelich

[†]Electronic address: shklyar@theo.physik.uni-giessen.de

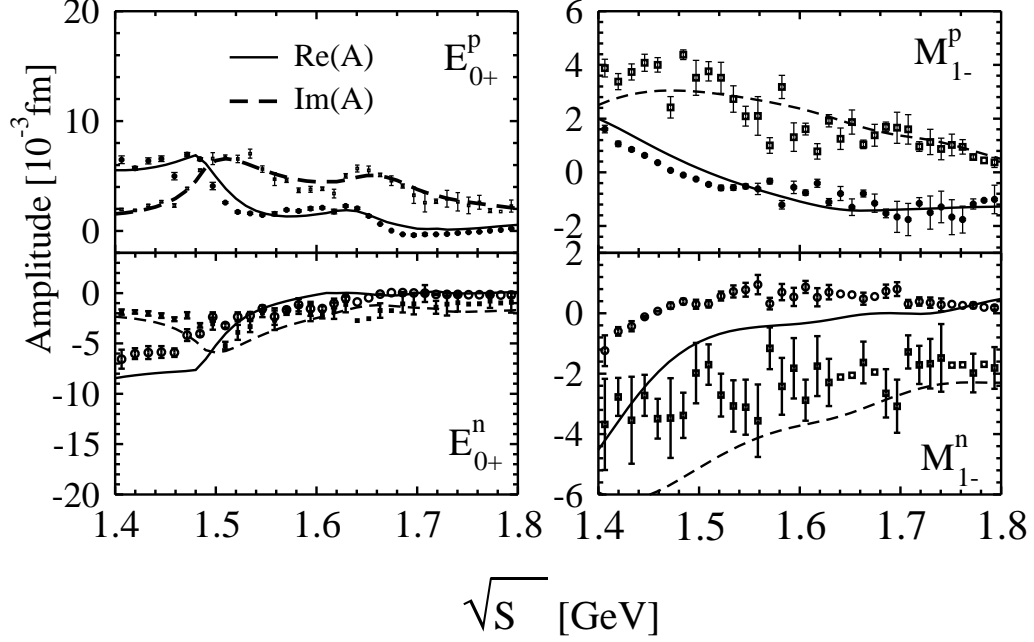


FIG. 1: Multipoles for pion photoproduction: proton (top) and neutron (bottom) respectively. Single energy amplitudes and energy-dependent solutions of the GW analysis [27] are shown by circles (real) and squares (imaginary) respectively.

In [19] ηn data were not included in the fit. In the present calculation we include the experimental data on the ratio $(d\sigma/d\Omega)_n/(d\sigma/d\Omega)_p$ of neutron to proton η photoproduction cross sections from [25]. These data cover the energy region 1.5...1.6 GeV but with large statistical errors. We include these data in our fit but multiply the original error bars by the factor of $\frac{1}{3}$. Above 1.6 GeV we include the preliminary data points of the total cross section $\gamma n \rightarrow \eta n$ from [26]. Starting from our best solution to the pion- and photon-induced reactions we perform an additional fit varying only the helicity decay amplitudes and ηNN^* -couplings of the isospin- $\frac{1}{2}$ resonances keeping all other parameters fixed. The obtained parameters are shown in Table I in comparison with the results from [19]. The variation of the ηNN^* -couplings leads in general to a modification of total widths of the resonances and affects the description of $\gamma p \rightarrow (\pi/\eta)p$ reaction. Hence a variation of the $A_{1/2}^p$ amplitudes was also allowed. However, only tiny changes in the proton helicity amplitudes are observed, indicating the reliability of the former calculations and their stability. The corresponding S_{11} - and P_{11} -multipoles for pion-photoproduction shown in Fig. 1 in comparison with the energy-independent solution from the analysis of the group at the George-Washington (GW) university [27]. At those energies, where the energy-independent solutions are not available, we have used the energy-dependent solutions from [27].

Including the new ηn data we find the most significant change in the neutron helicity amplitude for the N_{1535}^* resonance. The present value $A_{1/2}^n(S_{11}(1535)) = -74 \times 10^{-3} \text{GeV}^{-1/2}$ is much larger in magnitude than the one determined previously [19]. The change in the decay amplitude is necessary to describe the data [25] in the energy region 1.5...1.6 GeV, where the $S_{11}(1535)$ state gives the major contributions to η photoproduction. It leads to the ratio $R = A_{1/2}^n(S_{11}(1535))/A_{1/2}^p(S_{11}(1535)) \approx -0.8$ which is in line with the conclusions obtained in [21, 22, 23, 24]. At the same time, the changes in the properties of $S_{11}(1535)$ affect the real part of the E_{0+}^n multipole around 1.53 GeV, see Fig. 1. Interestingly, the same behaviour has also been found in the MAID calculations [22].

The second $S_{11}(1650)$ state has a large branching ratio to πN thereby a clear resonance behaviour is seen in the proton electric multipole E_{0+}^p at the energy 1.66 GeV. The effect from this resonance is much less pronounced in the E_{0+}^n multipole which points to a small magnitude of the corresponding neutron helicity amplitude. Note, that in the literature there is even no agreement on the sign of $A_{1/2}^n(S_{11}(1650))$, PDG [20]. We obtain $A_{1/2}^n(S_{11}(1650)) = -0.009 \text{GeV}^{-\frac{1}{2}}$ which is close to the value found by Arndt et. al. [27] and Penner and Mosel [18]. For the present discussion also the $P_{11}(1710)$ resonance is important but the properties of this state are not well determined, [20]. In

N^*	mass	Γ_{tot}	$\Gamma_{\pi N}$	$\Gamma_{\eta N}$	$A_{1/2}^p$	$A_{1/2}^n$	$A_{3/2}^p$	$A_{3/2}^n$
$S_{11}(1535)$	1526	136	34.4	56.2[+]	95	-74	—	—
	1526	136	34.4	56.1[+]	92	-13	—	—
	1535(10)	150(25)	45(10)	53(7)	90(30)	-46(27)	—	—
$S_{11}(1650)$	1664	133	71.9	2.5[-]	57	-9	—	—
	1664	131	72.4	1.4[-]	57	-25	—	—
	1655(15)	165(20)	72(22)	6(3)	53(16)	-15(21)	—	—
$P_{11}(1440)$	1517	608	56.0	—	-84	138	—	—
	1517	608	56.0	—	-84	138	—	—
	1440(30)	325(125)	65(10)	—	-65(4)	40(10)	—	—
$P_{11}(1710)$	1723	397	1.7	41.5[+]	-50	24	—	—
	1723	408	1.7	43.0[+]	-50	68	—	—
	1710(10)	150(100)	15(5)	6(1)	9(22)	-2(14)	—	—
$P_{13}(1720)$	1700	152	17.1	0.1[+]	-65	3	35	-1
	1700	152	17.1	0.2[+]	-65	1	35	-4
	1725(25)	225(75)	15(5)	4(1)	18(30)	1(15)	-19(20)	-29(61)
$P_{13}(1900)$	1998	369	24.5	5.4[-]	-8	12	0	23
	1998	404	22.2	2.5[-]	-8	-19	0	6
	1900	NG	26(6)	14(5)	-17	-16	31	2
$D_{13}(1520)$	1505	100	56.5	1.2[+]	-15	-64	146	-136
	1505	100	56.6	1.2[+]	-13	-70	145	-141
	1520(5)	112(12)	60(5)	0.2(0.04)	-24(9)	-59(9)	166(5)	-139(11)
$D_{13}(1950)$	1934	855	10.5	0.1[-]	11	26	26	-55
	1934	859	10.5	0.5[-]	11	40	26	-33
	2080	NG	NG	4(4)	-20(8)	7(13)	17(11)	-53(34)
$D_{15}(1675)$	1666	148	41.1	0.1[+]	9	-56	21	-84
	1666	148	41.1	0.3[+]	9	-56	21	-84
	1675(5)	146(16)	40(5)	0(1)	19(8)	-43(12)	15(9)	-58(13)
$F_{15}(1680)$	1676	115	68.3	0.0[+]	3	30	116	-48
	1676	115	68.3	0.0[+]	3	30	116	-48
	1685(5)	130(10)	68(3)	0(1)	-15(6)	29(10)	133(12)	-33(9)
$F_{15}(2000)$	1946	198	9.9	2.0[-]	11	9	25	-3
	1946	198	9.9	2.0[-]	11	9	25	-3
	2000	490(130)	8(5)	NG	—	—	—	—

TABLE I: Parameters of resonances considered in the present work. First line: parameters obtained in the present calculations. Second line: parameters are taken from our previous analysis [19]. In square brackets the sign of the ηNN^* coupling relative to the πNN^* coupling is given. Third line: values from PDG; in brackets estimated errors are given. NG - no average value in PDG is given. Helicity amplitudes are given in units of $10^{-3}\text{GeV}^{-\frac{1}{2}}$.

our previous study [19] this resonance was found to have a large branching ratio to ηN . In the present calculations the three states $S_{11}(1535)$, $S_{11}(1650)$, and $P_{11}(1710)$ give the major contributions to the $\pi^- p \rightarrow \eta n$ reaction, see Fig. 2. Above 1.65 GeV the destructive interference with the second $S_{11}(1650)$ resonance decreases the effective contribution to the S_{11} partial wave. A similar behaviour has also been found in the calculations of the rather different approach of the Jülich group [32]. The $P_{11}(1710)$ resonance together with the background contributions dominate the $\pi^- p \rightarrow \eta n$ reaction in the energy region under discussion developing a peak in the P_{11} -wave cross section around 1.7 GeV.

In the present calculations the η photoproduction on the proton is almost solely determined by the contribution from the S_{11} partial wave, see Fig. 3. Other partial wave cross sections have very small magnitudes, they are shown in the same figure for completeness. The situation changes for the η photoproduction on the neutron, Fig. 4. In the energy region 1.5...1.6 GeV the $S_{11}(1535)$ state strongly influences the production cross section. The second peak in the S_{11} -partial wave cross section around 1.66 GeV stems from the $S_{11}(1650)$ resonance. We also find an additional contribution coming from $P_{11}(1710)$. In our earlier photoproduction studies [18, 33] it has been concluded that strong interference effects must exist in this kind of reactions. Hence, the resonance contributions to the photoproduction

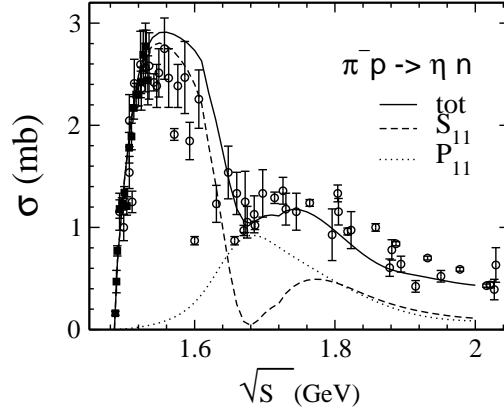


FIG. 2: $\pi^- p \rightarrow \eta n$ total and partial wave cross sections. The experimental data are taken from [28].

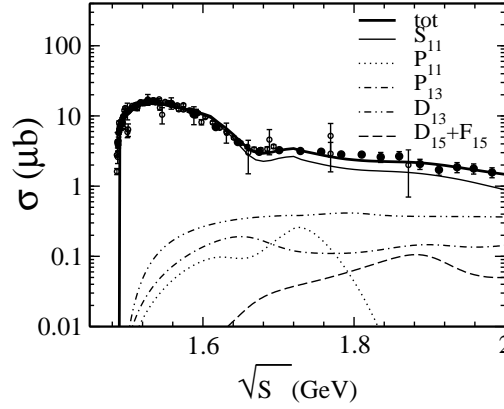


FIG. 3: $\gamma p \rightarrow \eta p$ total and partial wave cross sections. The experimental data are taken from [29, 30, 31].

depend strongly both on the sign and the magnitude of the N^* decay parameters. The calculated contribution from $P_{11}(1710)$ to the η photoproduction on the proton is small due to destructive interference [18]. Changing the sign of the $A_{1/2}^n(P_{11}(1710))$ amplitude enhances the effect of this resonance to the $\gamma n \rightarrow \eta n$ reaction.

The two kink structures seen in the S_{11} partial wave cross section at 1.61 GeV and 1.72 GeV in Fig. 4 are the threshold effects coming from the opening of the $K\Lambda$ and ωN channels, respectively. The effect from the ωN threshold is also seen in the $\gamma p \rightarrow \eta p$ cross section at 1.72 GeV, see Fig. 3. Note, that taking the final width of the ω meson into account would smear out this effect.

The overall magnitude of the second peak in the $\gamma n \rightarrow \eta n$ total cross section is very sensitive to the value of the neutron helicity amplitude of the $S_{11}(1650)$ and $P_{11}(1710)$ states. In the present calculations these parameters are constrained by the preliminary $\gamma n^* \rightarrow \eta n$ quasi-free total cross section data [26] which, however, has large statistical errors. These uncertainties might also affect the resonance helicity amplitudes. Therefore, in Fig. 5 we show the dependence of the cross section on the choice of parameters. Choosing $A_{1/2}^n(S_{11}(1650)) = -0.024 \text{ GeV}^{-\frac{1}{2}}$ changes the interference pattern in the S_{11} -partial wave and strongly decreases the magnitude of the second peak, see the dashed curve in Fig. 5. The contribution from the $S_{11}(1650)$ resonances becomes more pronounced when choosing a different sign for $A_{1/2}^n(S_{11}(1650))$. The same tendency is observed for the $P_{11}(1710)$ resonance: decreasing $A_{1/2}^n(P_{11}(1710))$ in magnitude enhances the overall contributions to the integrated cross section at 1.66 GeV. The differential cross sections calculated at 1.67 GeV using a different choice of the resonance parameters are shown in the right panel of Fig. 5. It is remarkable that in all cases mainly the magnitude of the backward angular distribution is affected but leaving the shape almost unchanged.

The experimental information on the $\gamma n \rightarrow \eta n$ reaction is commonly extracted from photo-nuclear reactions on the deuteron where the proton is taken to be a spectator. To take the effect of Fermi motion into account we have used the deuteron wave functions obtained with the Paris NN -potential [34]. Assuming $\sigma_{\eta n}^{\text{onshell}}(s) \approx \sigma_{\eta n}^{\text{offshell}}(s)$ the effect

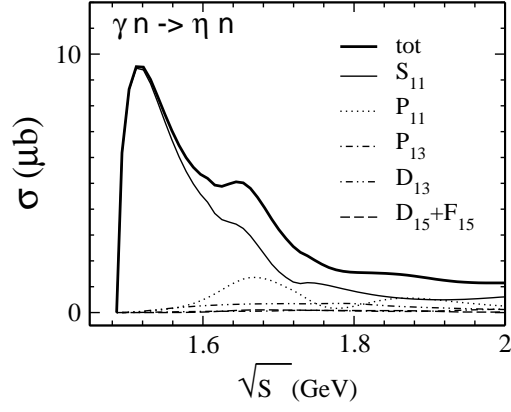


FIG. 4: $\gamma n \rightarrow \eta n$ total and partial wave cross sections. The kinks at 1.61 GeV and 1.72 GeV are the threshold effects coming from $K\Lambda$ and ωN .

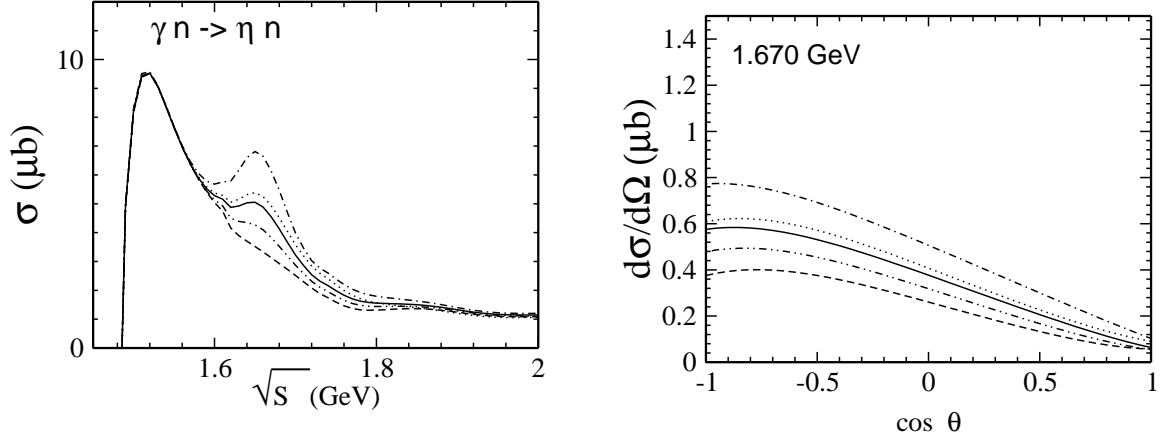


FIG. 5: $\gamma n \rightarrow \eta n$ total (left) and differential (right) cross sections calculated using the parameter set from Table I (solid line) and with different choice of the neutron helicity amplitudes for the $S_{11}(1650)$ and $P_{11}(1710)$ resonances: $A_{1/2}^n(S_{11}(1650)) = -24$ (dashed), $A_{1/2}^n(S_{11}(1650)) = -16$ (dashed-double-dotted), $A_{1/2}^n(S_{11}(1650)) = +3$ (dashed-dotted), $A_{1/2}^n(P_{11}(1710)) = +17$ (dotted), where the helicity amplitudes are given in units of $10^{-3} \text{GeV}^{-\frac{1}{2}}$.

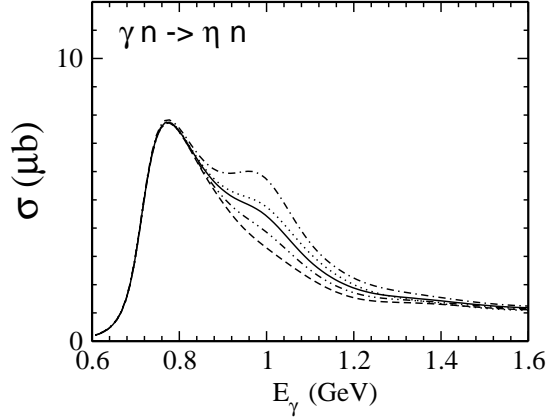


FIG. 6: The cross sections as in the left part of Fig. 5 but smeared out over the Fermi motion inside the deuteron. Notation is same as in Fig. 5.

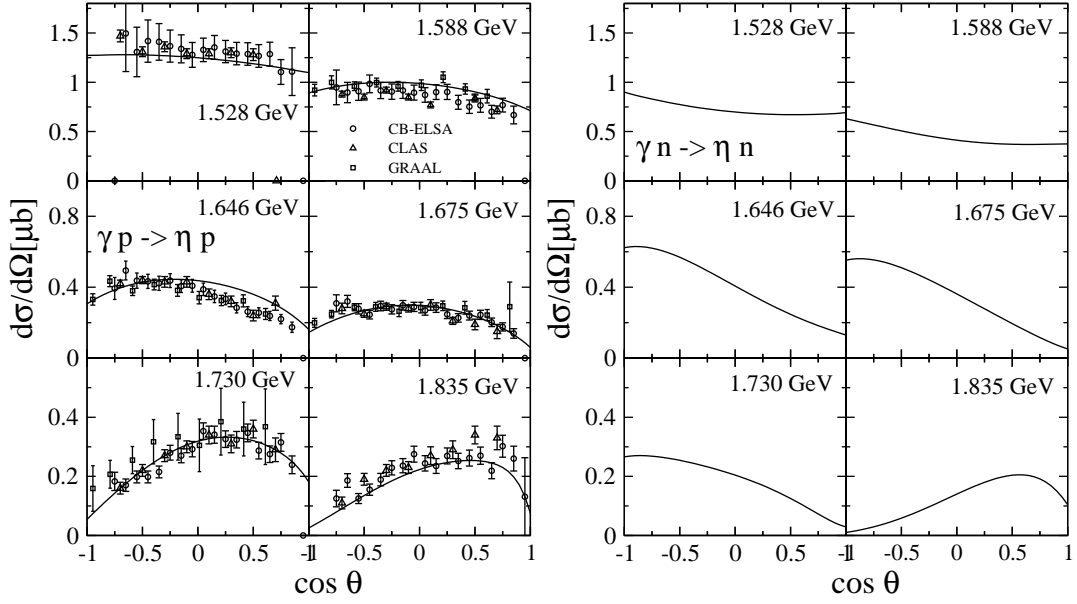


FIG. 7: $\gamma p \rightarrow \eta p$ (left) and $\gamma n \rightarrow \eta n$ (right) differential cross sections calculated for different total c.m. energies. The experimental data are taken from [29](CB-ELSA), [30](CLAS), and [31](GRAAL).

of the Fermi smearing can be approximately calculated by folding the elementary free space eta-n cross section by the deuteron momentum distribution

$$\sigma(E_\gamma) = \frac{1}{4\pi} \int d^3p \left(|u_s(p)|^2 + |u_d(p)|^2 \right) \sigma_{\eta n}(s^*), \quad s^* = (k_\gamma + p)^2, \quad (1)$$

where the information on the Fermi motion is carried by s- and d-state components $u_s(p)$ and $u_d(p)$ of the deuteron wave functions respectively.

The result is shown in Fig. 6. Once the Fermi motion is included the overall magnitude of the second resonance peak becomes less pronounced but is still visible. A narrow resonance proposed first in [14, 15] (and discussed more recently in [35]) or the contribution from the $D_{15}(1675)$ resonance proposed by Tiator [36] have been suggested as alternative explanations for the second peak found in the experimental data on the ηn photoproduction [12, 13]. From our calculations we conclude instead that coupled-channel and interference effects are a possible explanation for the structure seen in the experimental data. However, a fair statement is that at present the persisting experimental uncertainties translate into corresponding uncertainties in the theoretically derived parameters. In view of these problems a final answer must wait until more precise data are available. It is interesting to note that the experimental setup of the TAPS detector [11] apparently might minimize or even eliminate the effect of Fermi smearing from the data analysis. If this indeed could be achieved the observables shown in Fig.5 could be directly compared to experimental data.

The $\gamma p \rightarrow \eta p$ and $\gamma n \rightarrow \eta n$ differential cross sections are compared in Fig. 7. Similar to the photoproduction on the proton, the $\gamma n \rightarrow \eta n$ reaction is strongly influenced by the $S_{11}(1535)$ resonance contributions in the energy region from the threshold and up to 1.6 GeV. Due to the negative sign of the $A_{1/2}^n(S_{11}(1535))$ the angular distribution in the latter case has a different profile. A similar behaviour has been observed in [23]. At energies above 1.6 GeV the excitations of the $S_{11}(1650)$ and $P_{11}(1710)$ states give a strong effect which changes the angular distribution at forward angles. Above the 1.750 GeV the contributions from these states drop rapidly and the calculated distribution at 1.835 GeV becomes similar to that of $\gamma p \rightarrow \eta p$ reaction.

The calculated $(d\sigma/d\Omega)_n/(d\sigma/d\Omega)_p$ ratio is compared in Fig. 8 to the experimental data from [25]. Unfortunately, because of the large error bars no solid conclusion about the angular dependence can be drawn from this data. In the present calculations we find an almost symmetric angular distribution for this ratio with a minimum close to $\theta = 80^\circ$.

With the parameters fixed as just discussed we now make a prediction for the photon beam asymmetry. The photon beam asymmetry $\Sigma = \frac{d\sigma_\perp - d\sigma_\parallel}{d\sigma_\perp + d\sigma_\parallel}$ is shown in Fig. 9 as a function of scattering angle and fixed energies, where $d\sigma_\perp(d\sigma_\parallel)$ is a differential cross section of the $\gamma n \rightarrow \eta n$ reaction with the linearly polarized photons in horizontal (vertical) direction relative to the reaction plane. The calculated asymmetry is positive and has a maximum at forward angles at all energies under consideration.

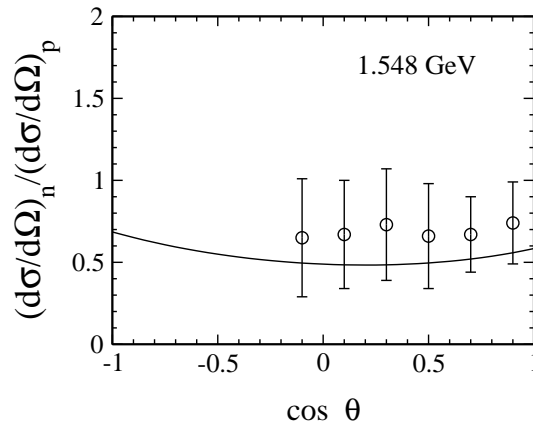


FIG. 8: Ratio of the η production cross sections on the proton and the neutron, as a function of the scattering angle and fixed total c.m. energy $\sqrt{s}=1.548$ GeV. The experimental data are taken from [25].

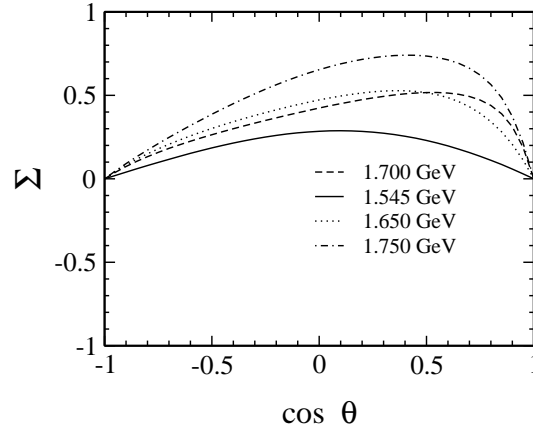


FIG. 9: Beam asymmetry as a function of the scattering angle and fixed total c.m. energies.

In summary, we have performed a new coupled-channel analysis of η photoproduction in the resonance energy region. To constrain the neutron helicity amplitudes of nucleon resonances we include in addition to pion photoproduction the experimental data on the $\gamma n \rightarrow \eta n$ reaction from [25, 26]. The inclusion of the ηn data lead to a significant modification of the neutron helicity amplitude of the $S_{11}(1535)$ resonance and to a lesser extent - of $S_{11}(1650)$. In line with the findings in [21, 22, 23, 24] we determine the ratio $A_{1/2}^n(S_{11}(1535))/A_{1/2}^p(N_{1535}^*) = -0.8$ which is required to describe the ηp - and ηn photoproduction data at energies close to the mass of the $S_{11}(1535)$ resonance. Our results show, that the second peak observed in the η photoproduction on the neutron at 1.66 GeV can be explained by the $S_{11}(1650)$ and $P_{11}(1710)$ resonance excitations without invoking an exotic narrow state. The differential cross section calculated at the position of the second peak shows a rise at backward direction. Above 1.75 GeV the contributions from these resonances decrease rapidly and the angular distribution becomes similar to that of the $\gamma p \rightarrow \eta p$ reaction. The precise measurements of the ηn differential cross section in the energy range 1.6...1.7 GeV might be decisive to distinguish between the present coupled-channels calculations and results of other theoretical approaches [15] and [35]. As an interesting by-product of our investigations we predict a beam asymmetry which has been measured at GRAAL and in presently being analyzed.

Acknowledgments

We thank I. Strakovsky and L. Tiator for the fruitful discussions and comments. The work is supported by Forschungszentrum Juelich.

-
- [1] T. Mart and C. Bennhold, Phys. Rev. **C61**, 012201 (2000), nucl-th/9906096.
 - [2] T. Mart and A. Sulaksono, Phys. Rev. **C74**, 055203 (2006), nucl-th/0609077.
 - [3] B. Julia-Diaz, B. Saghai, T. S. H. Lee, and F. Tabakin, Phys. Rev. **C73**, 055204 (2006), nucl-th/0601053.
 - [4] V. Shklyar, H. Lenske, and U. Mosel, Phys. Rev. **C72**, 015210 (2005), nucl-th/0505010.
 - [5] S. Capstick and W. Roberts, Phys. Rev. **D58**, 074011 (1998), nucl-th/9804070.
 - [6] S. Capstick and W. Roberts, Phys. Rev. **D49**, 4570 (1994), nucl-th/9310030.
 - [7] S. Capstick, Phys. Rev. **D46**, 2864 (1992).
 - [8] D. Diakonov, V. Petrov, and M. V. Polyakov, Z. Phys. **A359**, 305 (1997), hep-ph/9703373.
 - [9] R. L. Jaffe and F. Wilczek, Phys. Rev. Lett. **91**, 232003 (2003), hep-ph/0307341.
 - [10] B. Krusche et al., Phys. Lett. **B358**, 40 (1995).
 - [11] J. Weiss et al., Eur. Phys. J. **A16**, 275 (2003), nucl-ex/0210003.
 - [12] V. Kuznetsov (GRAAL), Phys. Lett. **B647**, 23 (2007), hep-ex/0606065.
 - [13] B. Krusche et al. (2006), nucl-th/0610011.
 - [14] R. A. Arndt, Y. I. Azimov, M. V. Polyakov, I. I. Strakovsky, and R. L. Workman, Phys. Rev. **C69**, 035208 (2004), nucl-th/0312126.
 - [15] Y. Azimov, V. Kuznetsov, M. V. Polyakov, and I. Strakovsky, Eur. Phys. J. **A25**, 325 (2005), hep-ph/0506236.
 - [16] V. Shklyar, G. Penner, and U. Mosel, Eur. Phys. J. **A21**, 445 (2004), nucl-th/0403064.
 - [17] G. Penner and U. Mosel, Phys. Rev. **C66**, 055211 (2002), nucl-th/0207066.
 - [18] G. Penner and U. Mosel, Phys. Rev. **C66**, 055212 (2002), nucl-th/0207069.
 - [19] V. Shklyar, H. Lenske, U. Mosel, and G. Penner, Phys. Rev. **C71**, 055206 (2005), nucl-th/0412029.
 - [20] W.-M. Yao, C. Amsler, D. Asner, R. Barnett, J. Beringer, P. Burchat, C. Carone, C. Caso, O. Dahl, G. D'Ambrosio, et al., Journal of Physics G **33** (2006), URL <http://pdg.lbl.gov>.
 - [21] C. Deutsch-Sauermann, B. Friman, and W. Norenberg, Phys. Lett. **B409**, 51 (1997), nucl-th/9701022.
 - [22] D. Drechsel, O. Hanstein, S. S. Kamalov, and L. Tiator, Nucl. Phys. **A645**, 145 (1999), nucl-th/9807001.
 - [23] N. C. Mukhopadhyay, J. F. Zhang, and M. Benmerrouche, Phys. Lett. **B364**, 1 (1995), hep-ph/9510307.
 - [24] W.-T. Chiang, S. N. Yang, L. Tiator, M. Vanderhaeghen, and D. Drechsel, Phys. Rev. **C68**, 045202 (2003), nucl-th/0212106.
 - [25] P. Hoffmann-Rothe et al., Phys. Rev. Lett. **78**, 4697 (1997).
 - [26] J. Jeagle, B. Krusche, and M. Kotulla (2006), private communication.
 - [27] R. A. Arndt, I. I. Strakovsky, and R. L. Workman, Phys. Rev. **C53**, 430 (1996), nucl-th/9509005.
 - [28] G. Penner, PhD thesis (in English), Giessen, available via <http://theorie.physik.uni-giessen.de> (2002).
 - [29] V. Crede et al. (CB-ELSA), Phys. Rev. Lett. **94**, 012004 (2005), hep-ex/0311045.
 - [30] M. Dugger et al. (CLAS), Phys. Rev. Lett. **89**, 222002 (2002).
 - [31] F. Renard et al. (GRAAL), Phys. Lett. **B528**, 215 (2002), hep-ex/0011098.
 - [32] A. M. Gasparyan, J. Haidenbauer, C. Hanhart, and J. Speth, Phys. Rev. **C68**, 045207 (2003), nucl-th/0307072.
 - [33] T. Feuster and U. Mosel, Phys. Rev. **C59**, 460 (1999), nucl-th/9803057.
 - [34] M. Lacombe et al., Phys. Lett. **B101**, 139 (1981).
 - [35] A. Fix, L. Tiator, and M. V. Polyakov (2007), nucl-th/0702034.
 - [36] V. Baru et al. (2006), nucl-th/0610011.